

Study of the selection rules of molecular polaritonic transitions by two-photon absorption spectroscopy

Kuidong Wang^{1*†}, Kalaivanan Nagarajan^{1‡}, Soh Kushida^{1,2}, Kulangara Sandeep^{1§}, Cyriaque Genet¹, Thomas W. Ebbesen^{1*}

¹University of Strasbourg, CNRS, ISIS & icFRC, 8 allée Gaspard Monge, 67000 Strasbourg, France.

²Faculty of Pure and Applied Sciences, and Tsukuba Research Center for Energy Materials Science (TREMS), University of Tsukuba, Tsukuba 305-8577, Japan

Corresponding Author

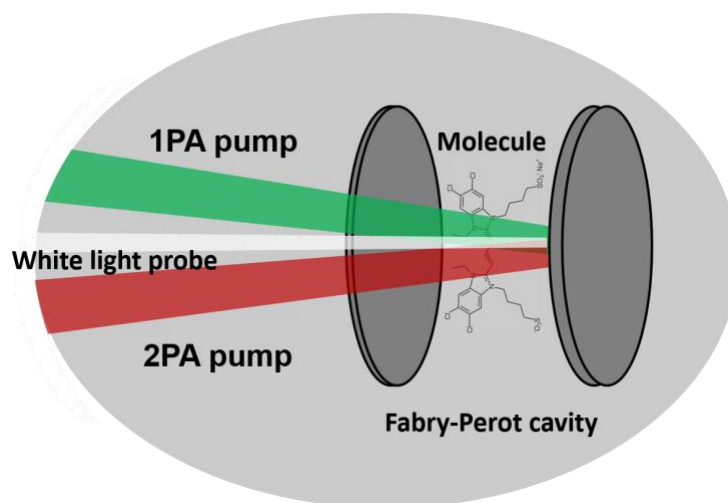
*Kuidong Wang: wangkuidong@xjtu.edu.cn

*Thomas W. Ebbesen: ebbesen@unistra.fr

ABSTRACT

Strong light-matter coupling is providing a new way to manipulate the physical and chemical properties of molecules. The study on intrinsic properties of the light-matter hybrid states (polaritonic states) in such coupled systems is of great importance in both molecular and optical sciences. Here, we explore the selection rules of the exciton-polaritons with respect to the symmetry of the coupled molecules. By using transient one-photon absorption (1PA) and two-photon absorption (2PA) spectroscopies, we find that the selection rules for the transition to the lower polaritonic state are different for 1PA and 2PA excitations strongly coupled rigid and symmetric J-aggregates, whereas they break down for softer flexible molecules with lower symmetry. The 0-delay transient spectra at 2PA can be different from those under 1PA condition, which reveals the co-existence of different excited states. Thus, the selection rules for the transition to polaritonic states and the excited state manifold are more complex than previously imagined and such studies should help to deepen the understanding of light-molecule strong coupling.

TOC GRAPHICS



KEYWORDS: strong light-matter coupling, polaritonic state, selection rules, symmetry of molecules, two-photon absorption

Strong coupling of light and molecules is paving a new way to control and modify the physical and chemical properties of organic materials.^{1, 2} In such coupled systems, the energy exchange rate between the excitonic/vibronic transition of molecules and the resonant mode of an optical cavity is faster than the dissipation processes of each constituent. Consequently, two polaritonic states $|P+\rangle$ and $|P-\rangle$, separated by the Rabi splitting energy $\hbar\Omega_R$, and $N-1$ dark states where N is the number of molecules coupled to the optical mode are generated. It should be recalled that these hybrid polaritonic states are formed even in the dark because the coupling occurs with the zero-point energy of the cavity mode, the so-called vacuum electromagnetic field. Because the polaritonic states can change the optical (photo-related) properties of the coupled systems in various aspects, e.g., it can enhance the optical nonlinearity³⁻⁵, the energy transfer rate⁶⁻⁹, triplet decay rate¹⁰, the rate of intersystem crossing¹¹, the diffusion coefficient of molecular excitons¹² and extend the lifetime of the excited polaritonic states^{13, 14}, in addition, it can also reduce the rate of photodegradation¹⁵ and photochemical reactivity¹⁶, which make it critical to probe their intrinsic properties by optical spectroscopy. Based on this, several useful tools, such as one-photon resonant absorption, emission and optical scattering spectroscopies, have been used to explore the static and dynamic properties of polaritons during past decades¹⁷⁻²³. Among these studies, some fundamental questions were raised due to the complexity of such hybrid systems. One such question is why it is difficult to populate the lower polaritonic state ($|P-\rangle$) when exciting an electronically strongly coupled (ESC) highly symmetric molecular J-aggregates at the resonant one-photon absorption wavelength of $|P-\rangle$, whereas such transition can be more easily accessed for flexible molecules of lower symmetry under strong coupling at the same excitation conditions.²² At the same time direct excitation of upper polariton ($|P+\rangle$) is easily achieved.²² Such

findings reflect the underlying selection rules for the polaritonic states which have not yet been understood and therefore invite further explorations.

Considering the transition probabilities in molecules, the selection rules are related to both the excitation process, e.g. whether via an one-photon (1PA) or two-photon absorption (2PA),²⁴ and the symmetry of the molecule. It is well known that for centrosymmetric molecules, parity selection rules are alternated for 1PA and 2PA processes, i.e., an one-photon forbidden electronic transition is allowed for two-photon excitation and *vice versa*.²⁵⁻²⁷ This remains usually true for molecules with no inversion symmetry but still characterized by strong mirror symmetries²⁸ such as TDBC (see below). In contrast, for molecules of lower symmetries, this alternation of the selection rules is expected to break down and consequently, the transition at the 2PA can reach the same state as that by the transition at 1PA.^{26, 27} It is recalled that in a 2PA process, two photons are simultaneously absorbed to excite the molecular system when the energy of the two photons is identical to or larger than the energy difference between the ground and the excited states.

Here, we study and compare the consequences of 1PA and 2PA of three different molecules in Fabry-Perot (FP) cavities under ESC. We find that the selection rules of the $|P\rangle$ transition are different for 1PA and 2PA excitations in strongly coupled rigid and symmetric J-aggregates where $|P\rangle$ can be populated by 2PA excitation but not by 1PA. Furthermore, the transient absorption spectra at 0 delay induced by 2PA are very different from those obtained with 1PA, indicating that 2PA leads to a different transient state. However, for molecules of lower symmetry, both 1PA and 2PA can populate the same excited state. These results, together with the difference between resonant excitation of $|P^+\rangle$ and $|P\rangle$ states, clearly point out that their selection rules are not the same. This should stimulate further studies to deepen our understanding of the electronic selection rules of polaritonic states of the strongly coupled molecules with different symmetries.

For the purpose of this study, we used the same molecules as those reported in our earlier work on action spectra of emission and transient absorption spectra under 1PA which already revealed differences between excitation of $|P+\rangle$ and $|P-\rangle$.²² These molecules are shown in Fig. 1. The symmetric molecule is TDBC (5,6-dichloro-2-[[5,6-dichloro-1-ethyl-3-(4-sulfobutyl)-benzimidazol-2-ylidene]-propenyl]-1-ethyl-3-(4-sulphobutyl)-benzimidazolium hydroxide, inner salt, sodium salt, Few Chemicals), as shown in Figure 1a (monomeric form). The absorption peak of the TDBC becomes sharp with the formation of J-aggregates, which results in longer lifetime

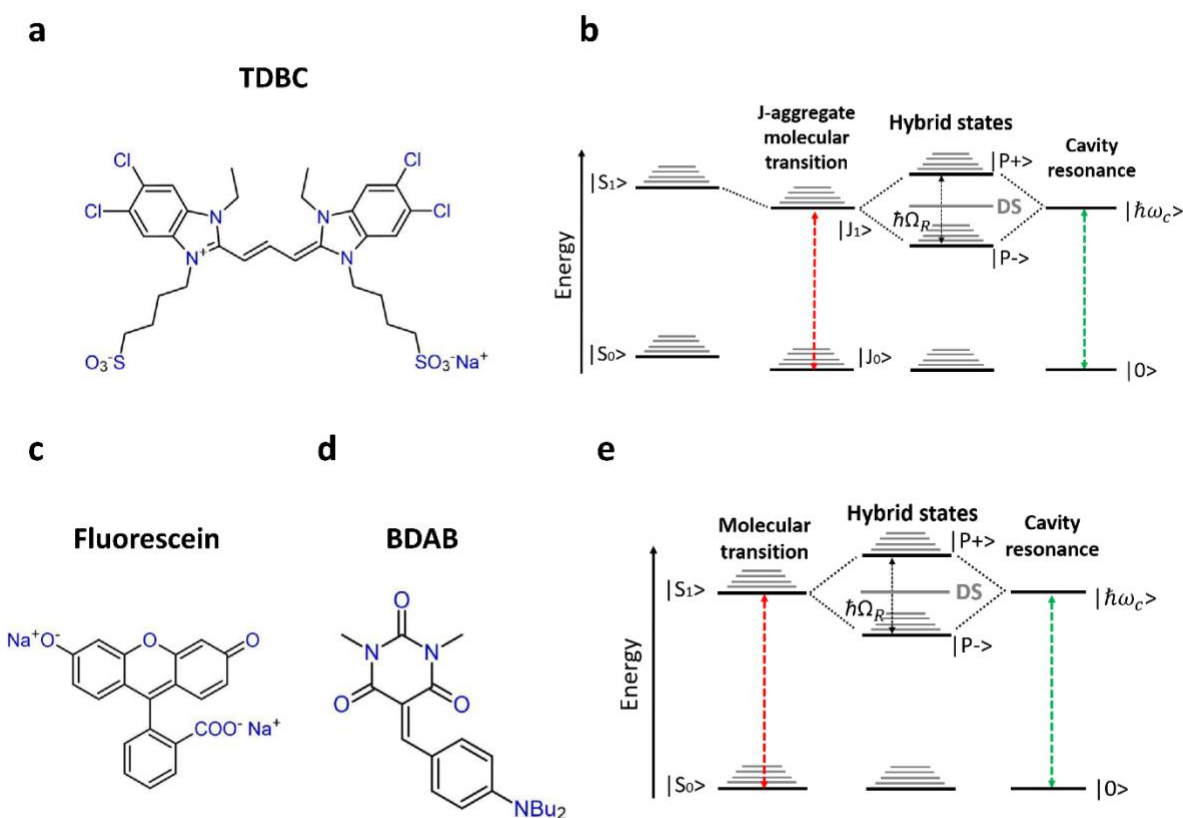


Figure 1. Strong light-matter coupling in organic molecules. (a) Chemical structure of the symmetric molecule (TDBC) monomer used in this work. (b) Schematic energy diagram of the electronic strong coupling between an exciton transition of J-aggregate dye and an optical mode of the cavity. (c) and (d) are chemical structures of quasi-symmetric (fluorescein) and asymmetric (BDAB) molecules, respectively. (e) Strong coupling between the exciton transition of monomers and the cavity resonance (adapted from Ref. 22). DS in both (b) and (e) denote dark states.

for the excitons.²⁹ Such J-aggregate can be easily formed in aqueous solutions, and is especially suitable for electronic strong coupling studies.^{20, 30, 31} The schematic of strong coupling between the excitons of J-aggregate and the cavity mode is presented in Figure 1b. We also studied fluorescein and BDAB [5-(4-(dibutylamino)benzylidene)-1,3-dimethylpyrimidine-2,4,6(1H,3H,5H)-trione].³² Their structures are presented in Figures 1c and 1d. Because fluorescein and BDAB have broad strong resonances, strong coupling with large Rabi splitting can easily be achieved (Figure 1e).

The linear optical response of the molecules and the corresponding strongly coupled systems are shown in Figure 2. The ESC is achieved by sandwiching a molecule-doped polymer film between two parallel metallic mirrors (FP cavity), with a thin top mirror along and a thick bottom mirror to enable reflective measurements for both the linear and nonlinear optical spectroscopies. The details of the sample preparation can be found in the Method part.

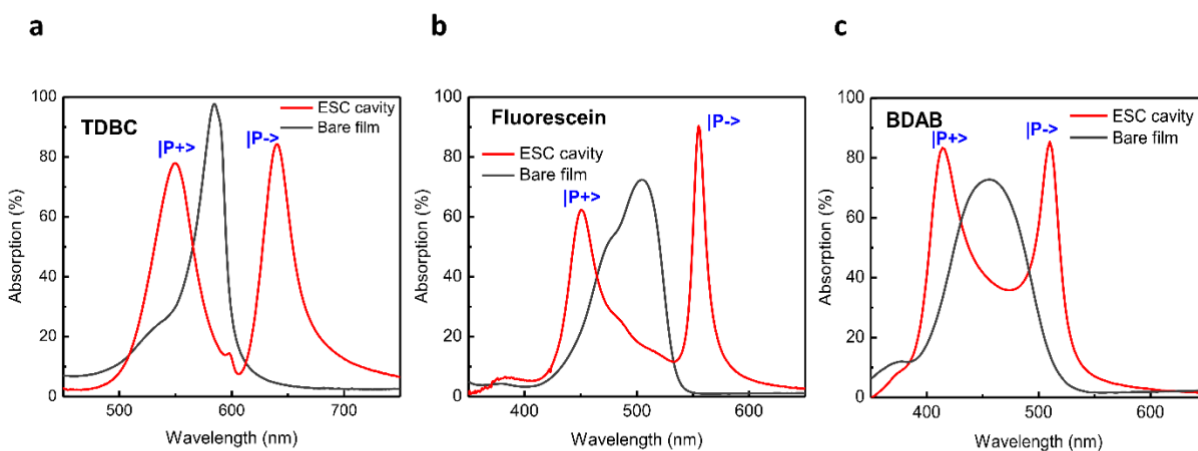


Figure 2. Linear optical response of the strongly coupled systems. Absorption spectra of the bare molecular film (molecule doped polymer film, black curves) and the ESC cavity (red curves) of (a) TDBC J-aggregate, (b) Fluorescein and (c) BDAB monomers measured at normal incidence. All samples are reflective type. Upper and lower polaritons of the coupled systems are denoted in all spectra.

The absorption peak of the excitonic mode of TDBC J-aggregate ($|J_1\rangle$) appears at 588 nm and has a linewidth of 84 meV. When this transition is strongly coupled to the optical mode of FP cavity, the formation of the ESC cavity results in the formation of two hybrid states, $|P+\rangle$ at 550 nm and $|P-\rangle$ at 640 nm, corresponding to a Rabi splitting of 317 meV, as shown in Figure 2a. When Fluorescein and BDAB monomers are strongly coupled at 504 nm and 456 nm, respectively, Rabi splittings of 521 and 556 meV were obtained (Figure 2b). It should be mentioned here, that we couple the first optical mode of the FP cavity in order to avoid the nonlinear optical effects of the cavity modes at the near-infrared range in 2PA measurements.

In order to avoid the discrepancy between the measured pump-probe differential transmittance spectra and the real transient absorption spectra of a transmissive cavity,²¹ reflective samples (the bottom mirror is highly reflective) were used in our study to estimate the transient absorption spectra by only recording the temporal evolving reflectance. The transient signals we measured are 1PA spectra when the excitation wavelengths close/equal to the absorption peaks of the sample. In the case of 2PA measurements, the pumping wavelengths are twice those used under 1PA.

For TDBC under ESC, 1PA excitation at multiple wavelengths that cover $|J_1\rangle$, $|P+\rangle$ and $|P-\rangle$ modes were investigated, as shown in Figure 3a at 0-delay between the pump and the probe. When we excite at the wavelength of $|P+\rangle$ ($\lambda_{|P+\rangle}$), a clear dip is observed for $|P+\rangle$ band due to the depopulation of the ground state (bleaching) while at the wavelength of $|P-\rangle$ ($\lambda_{|P-\rangle}$) the transient spectrum shows a combination of depopulation of the ground state, the absorption of the transient state plus stimulated emission, in agreement with earlier studies.^{21, 22} As the excitation wavelength increases, i.e., at 590 nm where $|J_1\rangle$ absorbs ($\lambda_{|J_1\rangle}$), the transient spectrum possesses a similar feature as that of the excitation at $\lambda_{|P+\rangle}$. This is reasonable because the excited upper

polariton or exciton can easily relax to the lower polaritonic state. The temporal evolution of the spectrum gives a 5.9-ps decay time accompanied by a weak differential absorption tail that decays over more than 100-ps (Figure 3b and Figure S1a). The spectral shape does not change with respect to the time delay, indicating that there is only one transient species. These results agree with previous measurements.²¹ As can be seen in the action spectrum as a function of pump wavelength,

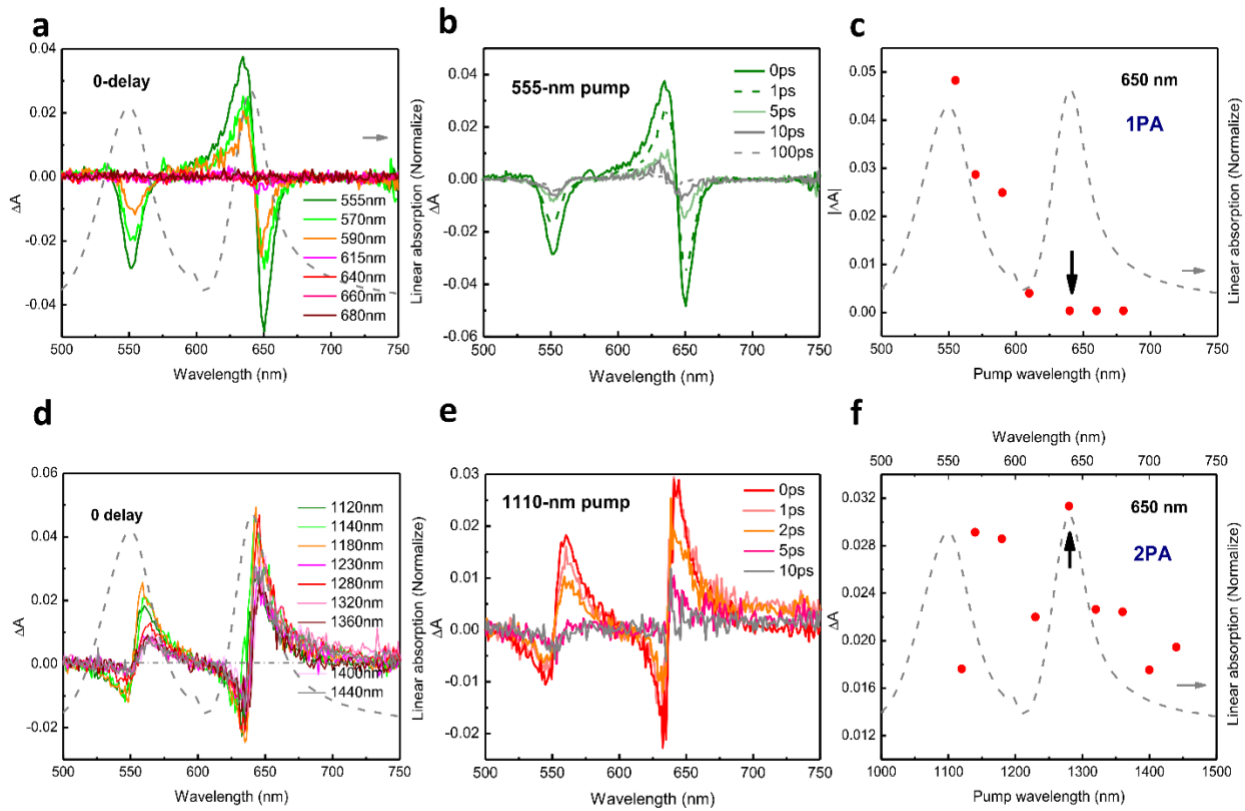


Figure 3. Nonlinear optical spectroscopy of TDBC J-aggregate under ESC. (a, d) Transient absorption spectra at zero delay, (b, e) temporal evolution of the transient spectra at typical pumping wavelengths, (c, f) action spectra recorded near $|P\rangle$ resonance (650 nm) under 1PA excitation (upper panel (a-c), $50 \mu\text{J}/\text{cm}^2$) and 2PA excitation (lower panel (e-f), $5 \text{ mJ}/\text{cm}^2$). Both the pump and probe beams are kept near normal incidence. The black arrows in (c) and (f) denote $\lambda_{|P\rangle}$ and $2\lambda_{|P\rangle}$, respectively, for the TDBC cavity. The dashed grey curves, which denote linear absorption spectrum of the ESC cavity for TDBC J-aggregate, are references for transient and action spectra in (a, c, d, f).

Figure 3c, no transient spectrum can be observed at the excitation region close to $\lambda_{|P-\rangle}$, which is consistent with the 1PA results of our earlier work.²² This indicates that no excited states can be accessed via resonant 1PA excitation at $\lambda_{|P-\rangle}$, therefore, such 1PA-induced electronic transition to $|P-\rangle$ must be forbidden. It still leaves the question of what is then the nature of the static $|P-\rangle$ absorption band (Figure 2a) as will be discussed further down.

As we mentioned above, symmetric molecules have different selection rules for 1PA and 2PA processes, thus, it is worth to carry out the 2PA excitation of the material under ESC to see if the transition to $|P-\rangle$ is allowed in that case. As displayed in Figures 3d, 3e and 3f, an excited state can be populated for all pumping wavelengths under 2PA, meanwhile the feature of 0-delay spectra are independent on 2PA-excitation wavelength. As can be seen in the spectrum, it is remarkably different from that obtained under 1PA. Furthermore, the spectral shape is unchanged with the decay of the transient process (Figure 3e), which suggests that the excited state reaches under 2PA is also dominated by one species, yet different from that induced by 1PA. The 3.1-ps decay time of the excited state induced by 2PA is shorter than that under 1PA (Figure S1). Clearly the selection rules for the transition to $|P-\rangle$ are very different for 1PA and 2PA excitations. The fact that 1PA and 2PA give rise to very different transient spectra with different lifetimes (5.9 ps versus 3.1 ps), suggests the co-existence of two distinct transient states each with their own selection rules. In other words, TDBC presents alternative selection rules for $|P-\rangle$ under 1PA and 2PA and very different for those of $|P+\rangle$. It should be noted that excitation of TDBC outside the cavity, just like the fluorescein and BDAB discussed below, give the same transient spectra under 1PA and 2PA (Figures S2, S3 and S4).

To further understand the influence of the molecular symmetry on selection rules of the strongly coupled systems, 1PA and 2PA transient spectra of molecules with lower symmetry under ESC were performed next. For fluorescein, the transient spectrum shows strong $|P\rangle$ stimulated emission near $\lambda_{|P\rangle}$ at 0 delay when exciting at wavelengths that cover $\lambda_{|P\rangle}$ and the uncoupled molecule absorption ($\lambda_{|S_1\rangle, \text{Fluorescein}}=504 \text{ nm}$) (Figure 4a). Interestingly, a relative weak $|P\rangle$

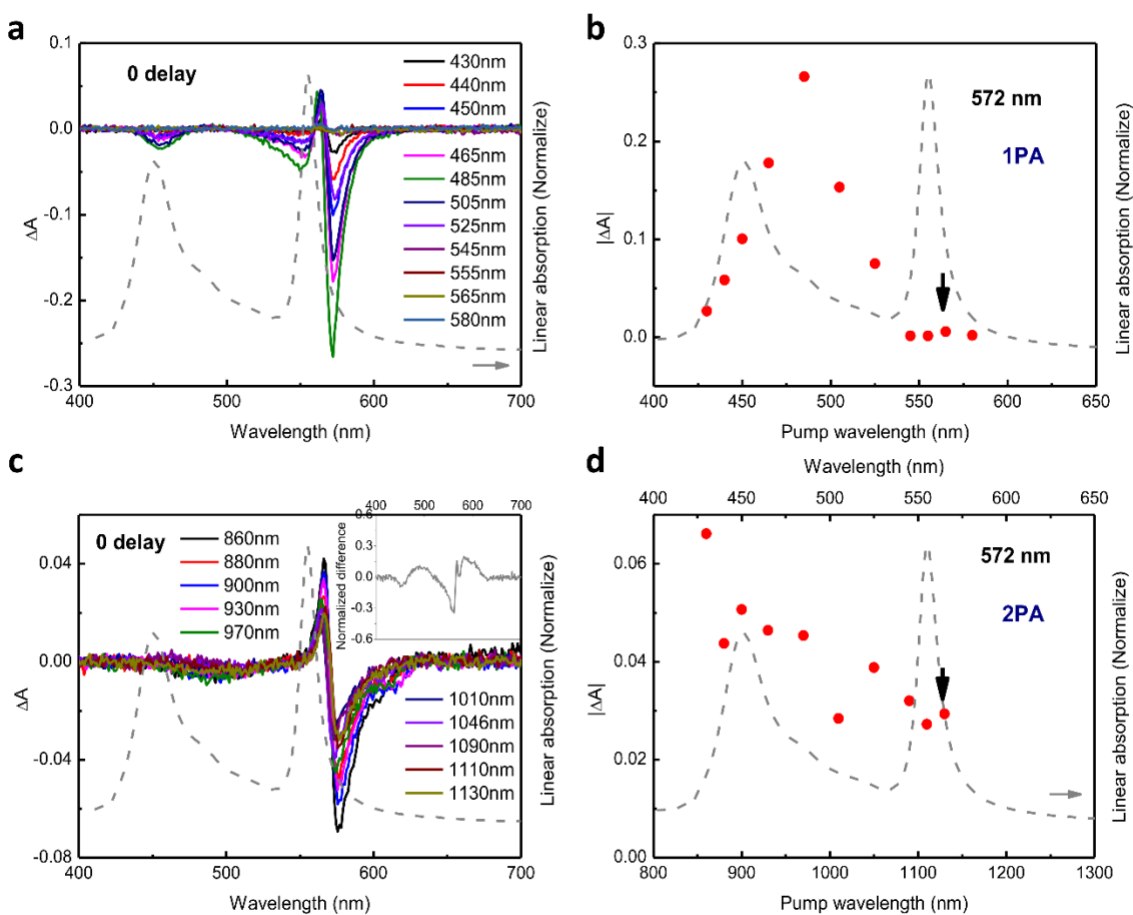


Figure 4. Nonlinear optical spectroscopy of fluorescein under ESC. (a, c) Transient absorption spectra at zero delay and (b, d) action spectra recorded near $|P\rangle$ resonance (572 nm) under 1PA excitation (upper panel (a, b)) and 2PA excitation (lower panel (c, d)). The black arrows in (b) and (d) denote $\lambda_{|P\rangle}$ and $2\lambda_{|P\rangle}$, respectively, for the fluorescein cavity. Inset of (c), normalized difference between 1PA and 2PA transient spectra. The dashed grey curves in each figure (linear absorption spectrum of fluorescein-assisted strong coupling) are references for transient and action spectra.

emission signal can also be observed when exciting at the wavelengths that close to $\lambda_{|P-\rangle}$ (Figure 4b), indicating that a direct excitation of the $|P-\rangle$ transition is possible in agreement with our earlier study.²² This is in contrast from the strictly forbidden $|P-\rangle$ transition of TDBC under 1PA. When excited by 2PA, remarkably $|P-\rangle$ emission can be measured for all pumping wavelengths, even at $2\lambda_{|P-\rangle}$, as displayed in Figures 4c and 4d. Such an intensive $|P-\rangle$ emission suggests that 2PA-induced electronic transition for $|P-\rangle$ is allowed, probably as a consequence of the lower symmetry. Considering that both 0-delay transient spectra and the dynamics of the strongly coupled fluorescein under 1PA and 2PA excitations are different (Inset of Figure 4c and Figure S5), the lifetime is 8.4 ps for 1PA and 2.0 ps for 2PA, these results show that the generated excited states are distinct in these conditions just as in the case of TDBC. Although the selection rules of $|P-\rangle$ transition for 1PA and 2PA excitations are still different, $|P-\rangle$ transition under 1PA excitation is not completely forbidden.

The BDAB molecule exhibits a clear $|P-\rangle$ stimulated emission around 520 nm and transient absorption for the 0-delay transient spectra when the pumping wavelength range covers $\lambda_{|P+\rangle}$, $\lambda_{|S_1\rangle, \text{BDAB}}$ (456 nm), as shown in Figure 5. This is similar to the results observed for that of coupled TDBC aggregate and fluorescein. However, when the excitation wavelengths are close to $\lambda_{|P-\rangle}$ (510 nm for BDAB ESC cavity), strong $|P-\rangle$ emission can also be observed (Figure 5a), unlike the other two molecules, reaching a maximum at the $\lambda_{|P-\rangle}$ transition, as shown in Figure 5b, in agreement with earlier findings.²² Similar transient spectra are obtained under 2PA, when the pumping wavelengths cover $2\lambda_{|P+\rangle}$ and $2\lambda_{|P-\rangle}$. Although the decay rate of the populated $|P-\rangle$ for 2PA is relatively faster than that for 1PA (Figure S6), the similar action spectra for 1PA and 2PA indicates that the electronic transition to $|P-\rangle$ is allowed for both 1PA and 2PA excitation conditions (Figures 5b and 5d).

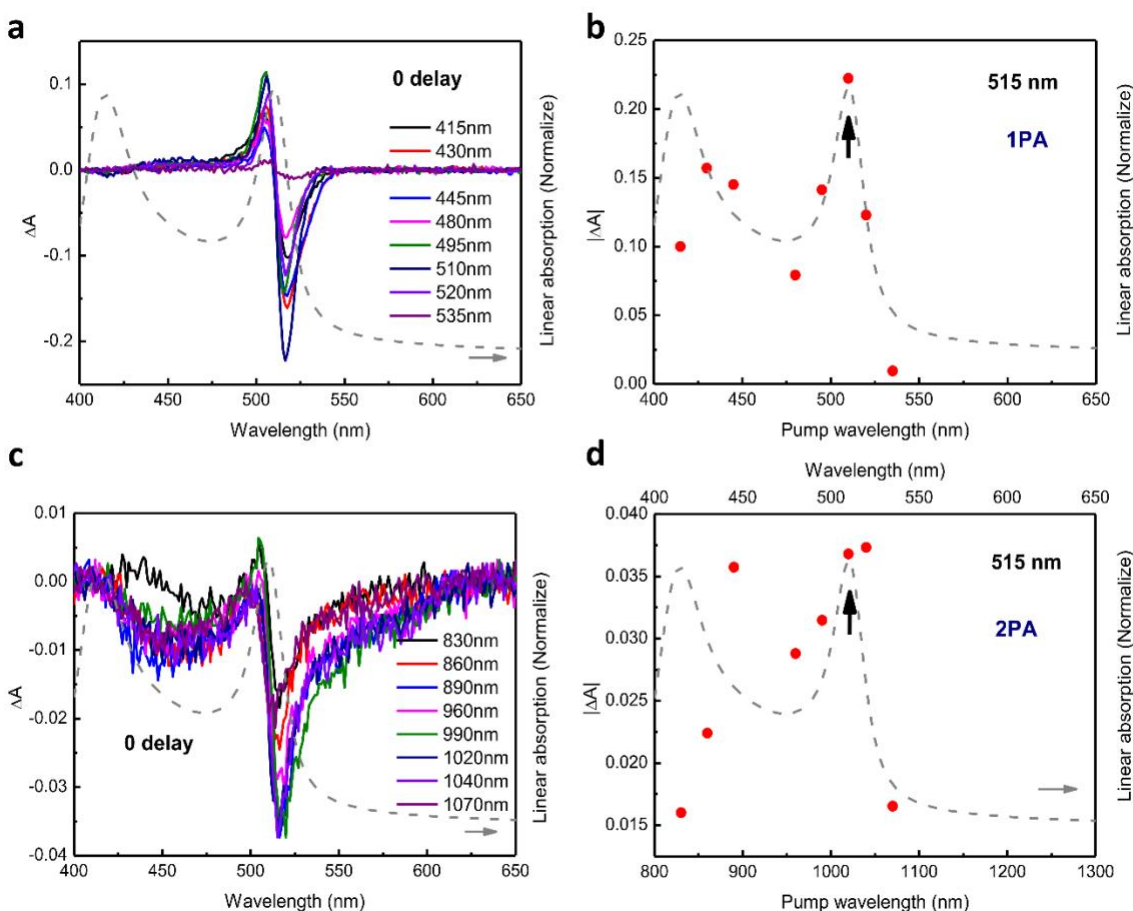


Figure 5. Nonlinear optical spectroscopy of BDAB molecules under ESC. (a, c) Transient absorption spectra at zero delay and (b, d) action spectra recorded near $|P-\rangle$ resonance (515 nm) under 1PA excitation (upper panel (a, b)) and 2PA excitation (lower panel (c, d)). The black arrows in (b) and (d) denote $\lambda_{|P-\rangle}$ and $2\lambda_{|P-\rangle}$, respectively, for the BDAB cavity. The dashed grey curves in each figure, which represent linear absorption spectrum of the ESC cavity for BDAB, are references for transient and action spectra.

The results from the study of the three molecules under ESC show that the selection rules are different for $|P-\rangle$ and $|P+\rangle$ and that the breakdown of the selection rules depends on the symmetry and rigidity of the molecules as expected from studies of molecular transitions.²⁴⁻²⁷ The comparison between 1PA and 2PA reveal that while direct excitation to $|P-\rangle$ can be quasi-forbidden by 1PA, it can be overcome by 2PA. However, surprisingly in that case, 1PA and 2PA

lead to different excited states as can be seen in the differential spectra and their distinct decay times. Furthermore, it also indicates that there is no crossing between these co-existing excited states, e.g. one excited state decaying into the other before returning to the ground state. It reveals the complexity of the potential energy surfaces induced by the presence hybrid light-matter states. These results then raise other questions, for instance what is the nature of the static absorption of $|P\rangle$ (a one photon process) if it doesn't lead to an excited state under 1PA? Is it just a dissipative classical mode, enhanced scattering²³ or a combination of the two? Only further studies, both theoretical and experimental, will help elucidate such questions. Understanding thoroughly the origin of these selection rules is important to realize the full potential of modifying and controlling properties under light-matter strong coupling.

EXPERIMENTAL METHODS

Preparation of the samples. As mentioned above, all the samples that used in our study are reflective type. Therefore, a thick bottom silver mirror (~150 nm) was first sputtered on an 1-mm quartz. Then, a molecule-doped polymer layer was spin coated from the corresponding molecule-polymer solution on top of the bottom mirror, and finally a 30-nm top silver mirror was sputtered on top of the polymer film to form a reflective Fabry-Perot cavity. For non-cavity cases, we only have bottom mirror and molecule-doped polymer film, without the top mirror. To obtain flat films as required for the FP cavity, poly(vinyl alcohol) (PVA) was selected to form polymer matrix for TDBC and fluorescein molecules, and poly(methyl methacrylate) (PMMA) was chosen for BDAB molecule. In addition, each molecule-polymer solution was made by mixing equal volume amount of molecule-solvent and polymer-solvent solutions. To realize strong coupling, the thickness of each molecule-doped polymer film was carefully selected in order to make the cavity resonances and the molecular absorption peaks overlap. The parameters of various molecule-solvent and polymer-solvent solutions and spin-coating speeds are listed in Table I.

Sample	Concentration of the molecule solution (wt%)	Concentration of the polymer solution (wt%)	Solvent	r.p.m. for spin coating

TDBC-PVA	0.5	5	water	1900
BDAB-PMMA	2	5	toluene	4000
Fluorescein-PVA	2	5	water	3600

Note: TDBC-PVA denotes TDBC doped PVA polymer film. High-purity water used here has a resistivity of $18.2 \text{ M}\Omega\cdot\text{cm}$ at $25 \text{ }^\circ\text{C}$ (Sartorius AG); The molar weight of PVA and PMMA are 205 000 and 120 000, respectively. The toluene is commercially available from the Sigma Aldrich company. The TDBC and fluorescein molecules are commercially available. BDAB can be synthesized as the procedures reported in Ref.²²

ASSOCIATED CONTENT

Supporting Information

The Supporting Information is available free of charge at ...

Supporting figures (The dynamics of the strongly coupled TDBC molecular system at 1PA and 2PA excitations, transient spectra for coupled Fluorescein and coupled BDAB molecules)

AUTHOR INFORMATION

Author contribution

T.W.E and K. W. conceived the study. K.W. prepared the samples with the help of K.N., S.K. and S.K., and performed all the optical measurements and the data analysis. All authors contributed to interpreting and discussing the results. C.G. and T.W.E supervised the project.

†Current address: Key Laboratory for Physical Electronics and Devices of the Ministry of Education & Shaanxi Key Lab of Information Photonic Technique, School of Electronic Science and Engineering, Xi'an Jiaotong University, Xi'an, 710049, China.

‡Current address: Department of Chemical Sciences, Tata Institute of Fundamental Research, Mumbai, 400005, India.

[§]Current address: Government Victoria College, Palakkad Research Center under the University of Calicut, Kerala India 678001

Notes

The authors declare no competing financial interest.

ACKNOWLEDGMENT

K. W. thank Tal Schwartz and Thibault Chervy for useful discussions. We acknowledge the support from the International Center for Frontier Research in Chemistry (icFRC, Strasbourg), the ANR Equipex Union (ANR-10-EQPX-52-01), the Labex NIE Projects (ANR-11-LABX-0058 NIE), CSC (ANR-10-LABX-0026 CSC), USIAS (Grant No. ANR-10-IDEX-0002-02) within the Investissement d'Avenir program ANR-10-IDEX-0002-02, ERC (project no 788482 MOLUSC), PlasHybrid (ANR-18-CE30-0014-02) and QuantERA project RouTe.

REFERENCES

1. Garcia-Vidal, F. J.; Ciuti, C.; Ebbesen, T. W., Manipulating matter by strong coupling to vacuum fields. *Science* 2021, 373, eabd0336.
2. Ebbesen, T. W., Hybrid Light–Matter States in a Molecular and Material Science Perspective. *Acc. Chem. Res.* 2016, 49, 2403-2412.
3. Wang, K.; Seidel, M.; Nagarajan, K.; Chervy, T.; Genet, C.; Ebbesen, T., Large optical nonlinearity enhancement under electronic strong coupling. *Nat. Commun.* 2021, 12, 1486.
4. Barachati, F.; Simon, J.; Getmanenko, Y. A.; Barlow, S.; Marder, S. R.; Kéna-Cohen, S., Tunable Third-Harmonic Generation from Polaritons in the Ultrastrong Coupling Regime. *ACS Photon.* 2018, 5, 119-125.
5. Xiang, B.; Wang, J.; Yang, Z.; Xiong, W., Nonlinear infrared polaritonic interaction between cavities mediated by molecular vibrations at ultrafast time scale. *Sci. Adv.* 2021, 7, eabf6397.

6. Coles, D. M.; Somaschi, N.; Michetti, P.; Clark, C.; Lagoudakis, P. G.; Savvidis, P. G.; Lidzey, D. G., Polariton-mediated energy transfer between organic dyes in a strongly coupled optical microcavity. *Nat. Mater.* 2014, 13, 712-719.
7. Zhong, X.; Chervy, T.; Wang, S.; George, J.; Thomas, A.; Hutchison, J. A.; Devaux, E.; Genet, C.; Ebbesen, T. W., Non-Radiative Energy Transfer Mediated by Hybrid Light-Matter States. *Angew. Chem. Int. Ed.* 2016, 55, 6202-6206.
8. Xiang, B.; Ribeiro, R. F.; Du, M.; Chen, L.; Yang, Z.; Wang, J.; Yuen-Zhou, J.; Xiong, W., Intermolecular vibrational energy transfer enabled by microcavity strong light–matter coupling. *Science* 2020, 368, 665-667.
9. Wang, M.; Hertzog, M.; Börjesson, K., Polariton-assisted excitation energy channeling in organic heterojunctions. *Nat. Commun.* 2021, 12, 1874.
10. Stranius, K.; Hertzog, M.; Börjesson, K., Selective manipulation of electronically excited states through strong light–matter interactions. *Nat. Commun.* 2018, 9, 2273.
11. Mukherjee, A.; Feist, J.; Börjesson, K., Quantitative Investigation of the Rate of Intersystem Crossing in the Strong Exciton–Photon Coupling Regime. *J. Am. Chem. Soc.* 2023, 145, 5155-5162.
12. Balasubrahmaniam, M.; Simkhovich, A.; Golombek, A.; Sandik, G.; Ankonina, G.; Schwartz, T., From enhanced diffusion to ultrafast ballistic motion of hybrid light–matter excitations. *Nat. Mater.* 2023, 22, 338-344.
13. Wang, S.; Chervy, T.; George, J.; Hutchison, J. A.; Genet, C.; Ebbesen, T. W., Quantum Yield of Polariton Emission from Hybrid Light-Matter States. *J. Phys. Chem. Lett.* 2014, 5, 1433-1439.
14. Wu, F.; Finkelstein-Shapiro, D.; Wang, M.; Rosenkampff, I.; Yartsev, A.; Pascher, T.; Nguyen-Phan, T. C.; Cogdell, R.; Börjesson, K.; Pullerits, T., Optical cavity-mediated exciton dynamics in photosynthetic light harvesting 2 complexes. *Nat. Commun.* 2022, 13, 6864.
15. Peters, V. N.; Faruk, M. O.; Asane, J.; Alexander, R.; Peters, D. a. A.; Prayakarao, S.; Rout, S.; Noginov, M. A., Effect of strong coupling on photodegradation of the semiconducting polymer P3HT. *Optica* 2019, 6, 318-325.
16. Munkhbat, B.; Wersäll, M.; Baranov, D. G.; Antosiewicz, T. J.; Shegai, T., Suppression of photo-oxidation of organic chromophores by strong coupling to plasmonic nanoantennas. *Sci. Adv.* 2018, 4, eaas9552.

17. Lidzey, D. G.; Bradley, D. D. C.; Virgili, T.; Armitage, A.; Skolnick, M. S.; Walker, S., Room Temperature Polariton Emission from Strongly Coupled Organic Semiconductor Microcavities. *Phys. Rev. Lett.* 1999, 82, 3316-3319.
18. Hakala, T. K.; Toppari, J. J.; Kuzyk, A.; Pettersson, M.; Tikkanen, H.; Kunttu, H.; Törmä, P., Vacuum Rabi Splitting and Strong-Coupling Dynamics for Surface-Plasmon Polaritons and Rhodamine 6G Molecules. *Phys. Rev. Lett.* 2009, 103, 053602.
19. Fofang, N. T.; Park, T.-H.; Neumann, O.; Mirin, N. A.; Nordlander, P.; Halas, N. J., Plexcitonic Nanoparticles: Plasmon–Exciton Coupling in Nanoshell–J-Aggregate Complexes. *Nano Lett.* 2008, 8, 3481-3487.
20. Aberra Guebrou, S.; Symonds, C.; Homeyer, E.; Plenet, J. C.; Gartstein, Y. N.; Agranovich, V. M.; Bellessa, J., Coherent Emission from a Disordered Organic Semiconductor Induced by Strong Coupling with Surface Plasmons. *Phys. Rev. Lett.* 2012, 108, 066401.
21. Schwartz, T.; Hutchison, J. A.; Léonard, J.; Genet, C.; Haacke, S.; Ebbesen, T. W., Polariton dynamics under strong light–molecule coupling. *ChemPhysChem* 2013, 14, 125-131.
22. George, J.; Wang, S.; Chervy, T.; Canaguier-Durand, A.; Schaeffer, G.; Lehn, J.-M.; Hutchison, J. A.; Genet, C.; Ebbesen, T. W., Ultra-strong coupling of molecular materials: spectroscopy and dynamics. *Faraday Discuss.* 2015, 178, 281-294.
23. Golombek, A.; Balasubrahmaniyam, M.; Kaek, M.; Hadar, K.; Schwartz, T., Collective Rayleigh Scattering from Molecular Ensembles under Strong Coupling. *J. Phys. Chem. Lett.* 2020, 11, 3803-3808.
24. Bonin, K. D.; McIlrath, T. J., Two-photon electric-dipole selection rules. *J. Opt. Soc. Am. B* 1984, 1, 52-55.
25. Craig, D. P.; Thirunamachandran, T., *Molecular quantum electrodynamics: an introduction to radiation-molecule interactions*. Courier Corporation: 1998.
26. Antonov, L.; Kamada, K.; Ohta, K.; Kamounah, F. S., A systematic femtosecond study on the two-photon absorbing D- π -A molecules– π -bridge nitrogen insertion and strength of the donor and acceptor groups. *Phys. Chem. Chem. Phys.* 2003, 5, 1193-1197.
27. De Boni, L.; Misoguti, L.; Zílio, S. C.; Mendonça, C. R., Degenerate Two-Photon Absorption Spectra in Azoaromatic Compounds. *ChemPhysChem* 2005, 6, 1121-1125.
28. Makarov, N. S.; Drobizhev, M.; Wicks, G.; Makarova, E. A.; Lukyanets, E. A.; Rebane, A., Alternative selection rules for one- and two-photon transitions in tribenzotetraazachlorin:

Quasi-centrosymmetrical π -conjugation pathway of formally non-centrosymmetrical molecule. *J. Chem. Phys.* 2013, 138, 214314.

29. Bricks, J. L.; Slominskii, Y. L.; Panas, I. D.; Demchenko, A. P., Fluorescent J-aggregates of cyanine dyes: basic research and applications review. *Methods Appl. Fluoresc.* 2018, 6, 012001.

30. Bellessa, J.; Bonnard, C.; Plenet, J. C.; Mugnier, J., Strong Coupling between Surface Plasmons and Excitons in an Organic Semiconductor. *Phys. Rev. Lett.* 2004, 93, 036404.

31. Tischler, J. R.; Bradley, M. S.; Bulović, V.; Song, J. H.; Nurmikko, A., Strong Coupling in a Microcavity LED. *Phys. Rev. Lett.* 2005, 95, 036401.

32. Canaguier-Durand, A.; Devaux, E.; George, J.; Pang, Y.; Hutchison, J. A.; Schwartz, T.; Genet, C.; Wilhelms, N.; Lehn, J.-M.; Ebbesen, T. W., Thermodynamics of Molecules Strongly Coupled to the Vacuum Field. *Angew. Chem. Int. Ed.* 2013, 52, 10533-10536.

Supporting Information for “Study of selection rules on molecular polaritons by two-photon absorption spectroscopy”

Kuidong Wang^{1*†}, Kalaivanan Nagarajan^{1‡}, Soh Kushida^{1,2}, Kulangara Sandeep^{1§}, Cyriaque Genet¹, Thomas W. Ebbesen^{1*}

¹University of Strasbourg, CNRS, ISIS & icFRC, 8 allée Gaspard Monge, 67000 Strasbourg, France.

²Faculty of Pure and Applied Sciences, and Tsukuba Research Center for Energy Materials Science (TREMS), University of Tsukuba, Tsukuba 305-8577, Japan

Corresponding Author

*Kuidong Wang: wangkuidong@xjtu.edu.cn

*Thomas W. Ebbesen: ebbesen@unistra.fr

[†]Current address: Key Laboratory for Physical Electronics and Devices of the Ministry of Education & Shaanxi Key Lab of Information Photonic Technique, School of Electronic Science and Engineering, Xi'an Jiaotong University, Xi'an, 710049, China.

[‡]Current address: Department of Chemical Sciences, Tata Institute of Fundamental Research, Mumbai, 400005, India.

[§]Current address: Government Victoria College, Palakkad Research Center under the University of Calicut, Kerala India 678001

Supporting figures

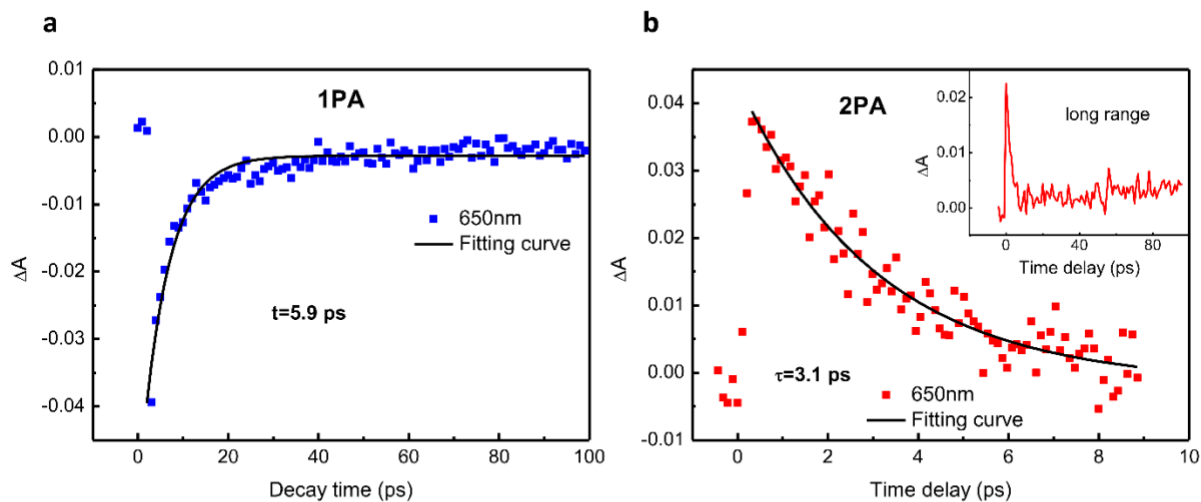


Figure S1. The dynamics of the strongly coupled TDDBC molecules at 1PA and 2PA excitations. (a) Temporal evolution of the $|P\rangle$ emission at 650 nm when excited at 555 nm (1PA) under a fluence of $50 \mu\text{J}/\text{cm}^2$. (b) Dynamics of the populated $|P\rangle$ at 650 nm when pumped at 1110 nm (2PA) under a fluence of $5 \text{ mJ}/\text{cm}^2$. Inset to (b), long range measurements for the dynamics of the 2PA-induced $|P\rangle$.

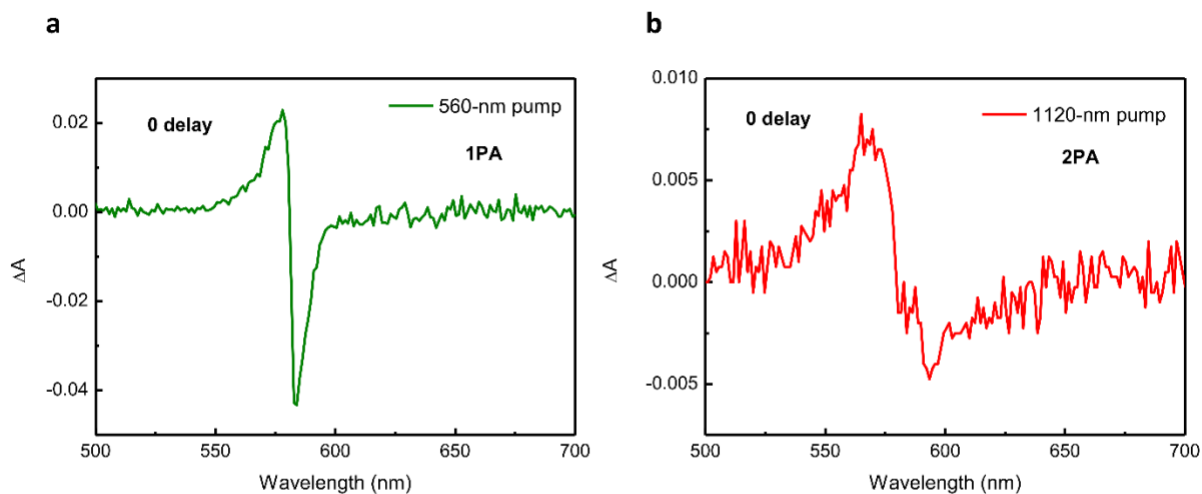


Figure S2. Transient absorption spectra of TDDBC J-aggregate outside the cavity. Zero-delay spectra under (a) 560-nm pump (1PA) and (b) 1120-nm excitation (2PA).

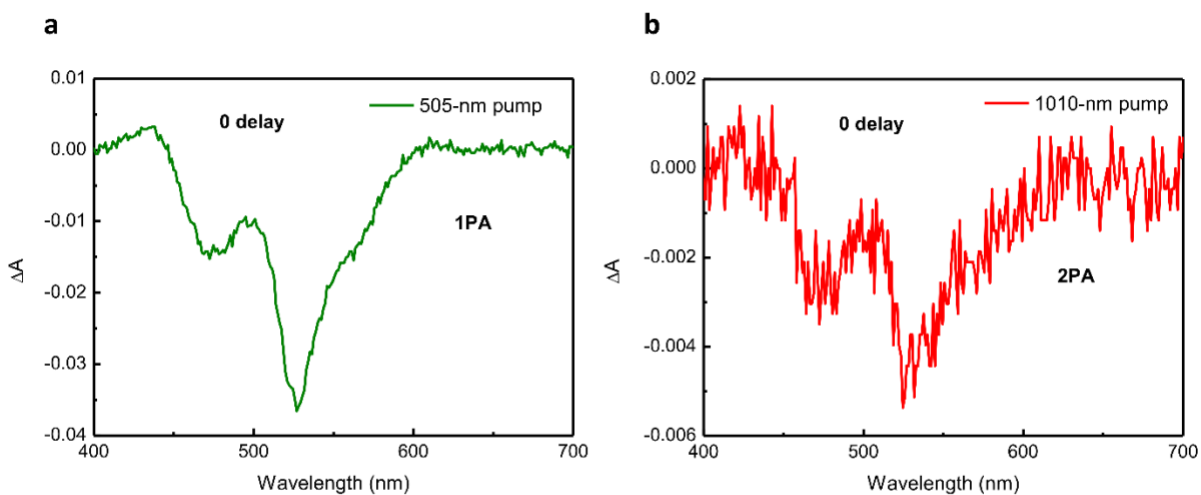


Figure S3. Transient absorption spectra of Fluorescein molecules outside the cavity. Zero-delay spectra under (a) 505-nm pump (1PA) and (b) 1010-nm excitation (2PA).

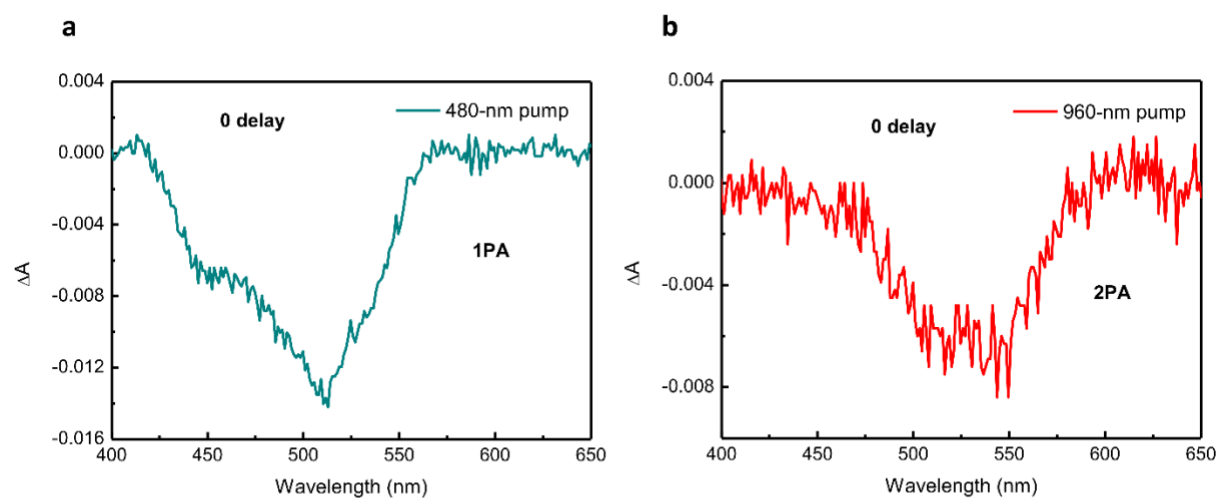


Figure S4. Transient absorption spectra of BDAB molecules outside the cavity. Zero-delay spectra under (a) 480-nm pump (1PA) and (b) 960-nm excitation (2PA).

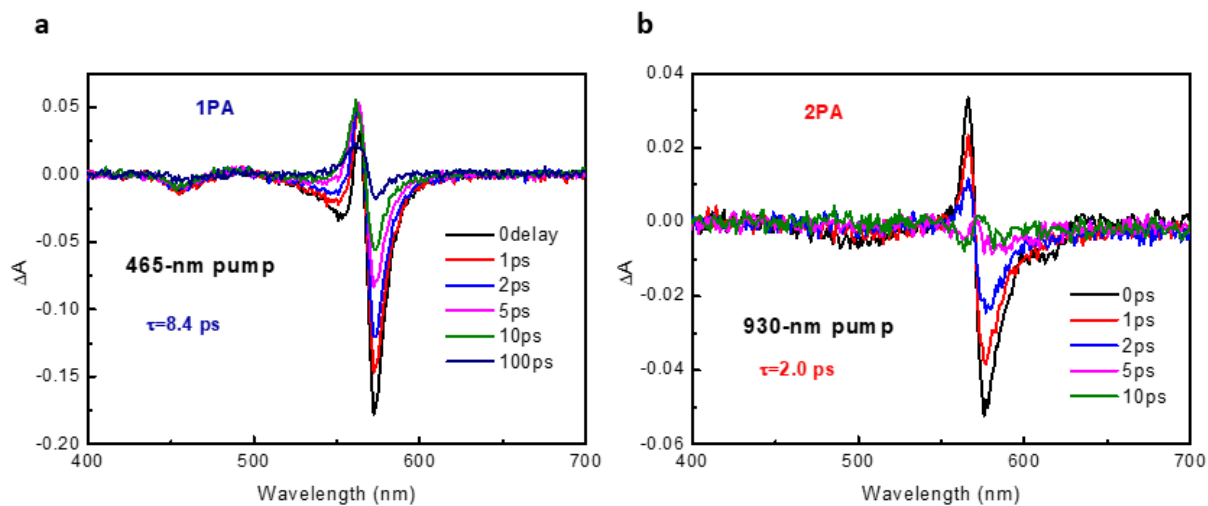


Figure S5. Temporal evolution of the absorption spectra for strongly coupled fluorescein under (a) 1PA (465-nm) and (b) 2PA (930-nm) excitations.

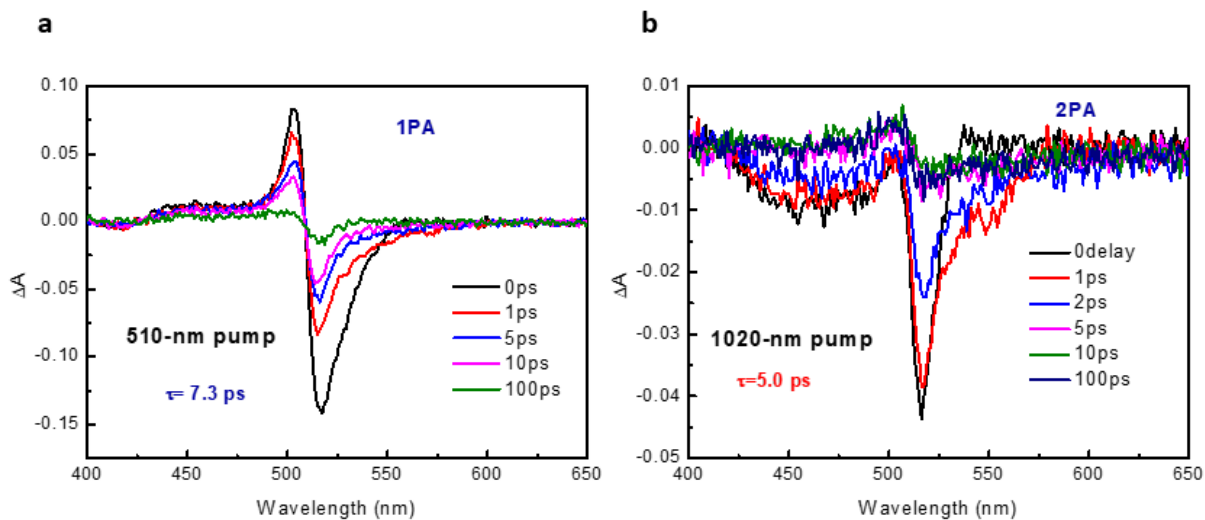


Figure S6. Transient absorption spectra with respect to time delay for BDAB molecules under ESC when excited by (a) 1PA (510-nm) and (b) 2PA (1020-nm) conditions.

